ELSEVIER

Journal of Chromatography A, 872 (2000) 1–21

JOURNAL OF CHROMATOGRAPHY A

www.elsevier.com/locate/chroma

Study on the accuracy of the elution by characteristic point method for the determination of single component isotherms

Kanji Miyabe[a,b], Saad Khattabi[b,c], Djamel E. Cherrak[a,b], Georges Guiochon[a,b,*]

[a] *Department of Chemistry, The University of Tennessee, Knoxville, TN 37996-1600, USA*

[b] *Division of Chemical and Analytical Sciences, Oak Ridge National Laboratory, Oak Ridge, TN 37831-6120, USA*

[c] *Department of Food Science and Technology, The University of Tennessee, Knoxville, TN 37901-1071, USA*

Received 21 July 1999; received in revised form 22 November 1999; accepted 25 November 1999

Abstract

The accuracy of the method of elution by characteristic point (ECP) used to determine single component isotherms was studied numerically. Overloaded elution peaks were calculated using the equilibrium-dispersive model of nonlinear chromatography while varying the four parameters, i.e., the number of theoretical plates, the dimensionless Langmuir equilibrium constant, the retention and the loading factor, involved in the fundamental equations of the problem. Single component isotherms were estimated by analyzing the diffuse profile of the elution peaks by the ECP method. Similar results were obtained with the transport-dispersive model. The comparison of these calculated isotherms with the initial Langmuir isotherms provided detailed information on the influence of the mass transfer resistances on the accuracy of the isotherms afforded by the ECP method. The systematic error made on the isotherms depends on the experimental conditions, described by the four parameters. It is expected that this error could be eliminated by correcting the influence of nonequilibrium in the column on the basis of results of the nondimensional calculations. The concentration range of the objective isotherm which can be determined by the ECP method can also be predicted by numerical calculations. The usefulness of the correction strategy and the prediction of the concentration range were experimentally demonstrated.

Keywords: Adsorption isotherms; Characteristic point method; Mathematical modelling

1. Introduction

Equilibrium isotherm is one of the most important characteristics of adsorption phenomena [1,2]. Concentration profiles in various mass transfer operations, e.g., elution peaks in chromatography, depend first and foremost on the thermodynamic properties of the phase equilibrium, especially at high concentrations. Numerous methods were developed for the experimental determination of single component and of competitive isotherms [1–3].

The frontal analysis (FA) method is the most basic strategy of isotherm determination. It is applied irrespective of the column efficiency. It has two great advantages. Band self-sharpening takes place if the isotherm is convex toward the axis of amounts adsorbed, making the method effective for the accurate determination of equilibrium isotherms. Detector calibration is unnecessary. In connection with the FA method, Kawai [4] proposed an ingenious method by which the two Langmuir parameters and an overall

*Corresponding author.

0021-9673/00/$ – see front matter
PII: S0021-9673(99)01266-2

mass transfer coefficient could simultaneously be estimated from the width of the mass transfer zones of the breakthrough and desorption curves. Golshan-Shirazi and Guiochon [5] developed the convenient retention time method for the determination of the Langmuir parameters. When the phase equilibrium can be represented by a simple Langmuir isotherm, its two parameters can be derived from the retention times of two peaks recorded at infinite dilution and under overloaded conditions, if using a column of relatively high efficiency.

In pulse methods, a small perturbation pulse is injected into the mobile phase after equilibrium is achieved between the stationary phase and a stream of mobile phase containing the solute at a given concentration, held constant during a measurement. A pulse response peak is detected at a retention time corresponding to the slope of the tangent to the equilibrium isotherm at the solute concentration. Like the FA method, the pulse method needs no detector calibration. Peak spreading due to mass transfer resistances in the column has little influence on equilibrium data because only the retention time of the peak is measured. This time is not affected by the mass transfer resistances in the column [6–8]. However, a large-size perturbation-pulse must often be introduced because of limited detector sensitivity close to its saturation. It was pointed out that the size of the perturbation pulse may significantly influence the result of the measurement [9]. In the FA and pulse methods, only one data point of the objective isotherm is derived from each experimental determination. As many as possible breakthrough curves or pulse response peaks must be successively recorded by changing the solute concentration in the feed solution in order accurately to determine the equilibrium isotherm. Accordingly, a rather large amount of the compound studied is necessary. These are the main disadvantages of the two methods.

These disadvantages are overcome by the method of FA by characteristic point (FACP). The profile of the diffuse rear boundary of a desorption curve reflects the properties of the corresponding equilibrium isotherm. The elution volume (V_i) of a solute concentration (C_i) gives one point of the objective isotherm. The amount of solute adsorbed (q_i) at equilibrium with C_i can be calculated from V_i and C_i. Many isotherm points in the concentration range between 0 and the solute concentration (C_0) in the feed solution can be simultaneously obtained from only one desorption profile. In the method of elution by characteristic point (ECP), the diffuse profile of an overloaded elution peak is similarly analyzed instead of the diffuse rear boundary in the FACP method. An objective isotherm in the concentration range between 0 and a value close to the apical concentration can be determined as with the FACP method. A large size pulse must be injected to determine the isotherm in a wide concentration range. However, the amount of compound used is small compared with the that needed with the FA or pulse methods.

In FACP and ECP, the elution profile analysis assumes that local equilibrium is reached everywhere in the column during the elution process. The influence of axial dispersion along the column and of the mass transfer resistances between stationary and mobile phase on peak broadening is neglected. So, in order to obtain reasonably accurate data, it is required to use a column having a relatively high efficiency. Guan et al. [10] studied numerically the accuracy and precision of the ECP method. They showed that the column efficiency should exceed 2000 and preferably be close to 5000 theoretical plates. Jacobson et al. [9] pointed out that the potential drawback of FACP and ECP was the absence of a correction process for the band spreading due to mass transfer resistances. Conversely, the FACP and ECP methods could be used with low efficiency columns if there were a correction procedure for band spreading phenomena in the column.

The applicability of the ECP method depends on the column efficiency and the degree of curvature of the objective isotherm. The curvature of the isotherm in an adsorption system rests on both the coefficients of the objective isotherm and the solute concentration (C_0) in the feed solution. The maximum concentration must be high to allow the determination of the isotherm in a wide range of concentrations. The loading factor (L_f, the ratio of the sample size to the column saturation capacity) depends on C_0, the volume of feed solution injected, the amount of stationary phase, and its saturation capacity. The amount of stationary phase is correlated with the column size, that is, in part, to its efficiency. The saturation capacity is a function of the objective isotherm. In conclusion, the adaptability of the ECP method and the concentration

range accessible by the ECP method depend on several parameters of the adsorption system, such as the column efficiency, its size, the coefficients of the objective isotherm, and the L_f, parameters which are correlated together. This makes it difficult to decide on the validity of the ECP method.

The first aim of this study is systematically to study the applicability of ECP under various conditions by using nondimensional calculations and to propose a correction procedure allowing for the influence of mass transfer resistances on the systematic error made on single component isotherms obtained by ECP. This information is useful for extending the adaptability of ECP. Our second goal was to demonstrate the validity of the correction procedure for improving the accuracy of single component isotherm obtained by ECP.

2. Theory

The diffuse profile of an overloaded elution peak and of the rear boundary of a desorption curve were calculated using the equilibrium-dispersive model. The mass balance equation of the equilibrium model is written

$$\frac{\partial C}{\partial t} + F \cdot \frac{\partial q}{\partial t} + u \cdot \frac{\partial C}{\partial z} = 0 \tag{1}$$

where C and q are the mobile and stationary phase concentrations, respectively, t is the time, z the length along the column, F the phase ratio, and u the mobile phase velocity. This equation can be modified easily to calculate the profiles predicted by the equilibrium-dispersive model by including the proper amount of numerical dispersion [1] (see calculation method later in this section). Then, the equation is rewritten in nondimensional form as follows [1]

$$\frac{\partial C_d}{\partial Z_d} + \frac{\partial Q_d}{\partial T_d} + \frac{1}{F\beta} \cdot \frac{\partial C_d}{\partial T_d} = 0 \tag{2}$$

with

$$C_d = \frac{C}{C_0}, \quad Q_d = \frac{q}{q_0}, \quad Z_d = \frac{zu}{D_a},$$

$$T_d = (t - \frac{L}{u}) \cdot \frac{u^2}{D_a F \beta}, \quad F = \frac{1-\varepsilon}{\varepsilon},$$

$$\beta = \frac{q_0}{C_0}$$

where C_d and C are the dimensionless and actual mobile phase concentrations, respectively, Q_d and q the dimensionless and actual solid-phase concentrations, respectively, C_0 the concentration of the feed solution, q_0 the amount adsorbed in equilibrium with C_0, Z_d and z the dimensionless and actual longitudinal distance, respectively, u the linear velocity of the mobile phase, D_a the apparent axial dispersion coefficient, T_d and t the dimensionless and actual time, respectively, L the column length, F the phase ratio, ϵ the total void fraction of the column, and β the ratio of q_0 to C_0.

The equilibrium was assumed to be represented by the Langmuir isotherm

$$q = \frac{q_s K_L C}{1 + K_L C} \tag{3}$$

where q_s is the saturation capacity and K_L the equilibrium constant, exponentially related to the adsorption energy. The nondimensional form of the Langmuir equation is as follows

$$Q_d = \frac{C_d}{r + (1-r)C_d} \tag{4}$$

where

$$r = \frac{1}{1 + K_L C_0} \tag{5}$$

Numerical calculations were made using the forward–backward finite difference scheme, with the following integration increments for Z_d and T_d [1]

$$dZ_d = 2 \tag{6}$$

$$dT_d = \frac{4(1+k')}{rk'} \tag{7}$$

where k' is the retention factor. The initial and boundary conditions are as follows

$$\begin{array}{lll} T_d = -(T_{d,0} + T_{d,p}), & Z_d > 0; & C_d = 0, \quad Q_d = 0 \\ -(T_{d,0} + T_{d,p}) < T_d < -T_{d,0}, & Z_d = 0; & C_d = 1 \\ T_d > -T_{d,0}, & Z_d = 0; & C_d = 0 \end{array} \tag{8}$$

with

$$T_{d,0} = \frac{2N}{rk'} \tag{9}$$

$$T_{d,p} = \frac{2NL_f}{1-r} \tag{10}$$

where $T_{d,0}$ is the dimensionless hold-up time, $T_{d,p}$ the dimensionless time width of the injected pulse (assumed to have a rectangular profile), N the number of theoretical plates of the column, and L_f the loading factor. The latter two parameters are given by

$$Pe_L = \frac{Lu}{D_a} = 2N \tag{11}$$

$$L_f = \frac{n}{SL(1-\varepsilon)q_s} \tag{12}$$

where Pe_L is the column Peclet number, S the cross-sectional area, L the length of the column, and n the amount of solute injected.

In the nondimensional equations of the chromatographic problem, there are only four dimensionless parameters, N, r, k', and L_f. They all influence the accuracy of the isotherm parameters estimated by the ECP method. For example, the influence of r on the diffuse profile of the rear boundary of FACP curves is illustrated in Fig. 1. The nonlinear behavior of the isotherm and the degree of tailing of the rear boundary both increase with decreasing r. The influence of each parameter on the systematic error made on the objective isotherm by the ECP method was calculated by varying successively each parameter at constant values of the other ones.

In this study, numerical calculations were carried out using mainly the equilibrium-dispersive model of chromatography. We also compared the results of similar calculations based on the equilibrium-dispersive model and on various transport-dispersive models. We confirmed that the same profiles were obtained for either overloaded elution peaks or breakthrough curves with both models, as described in the following. In the lumped kinetic model [1], the mass balance and the kinetic equations are written as follows

$$\frac{\partial C}{\partial t} + F \cdot \frac{\partial q}{\partial t} + u \cdot \frac{\partial C}{\partial z} = D_L \cdot \frac{\partial^2 C}{\partial z^2} \tag{13}$$

$$\frac{\partial q}{\partial t} = k_m(q^* - q) \tag{14}$$

where D_L is the axial dispersion coefficient, k_m the mass transfer rate coefficient, and q^* the concentration of the solute in the stationary phase in

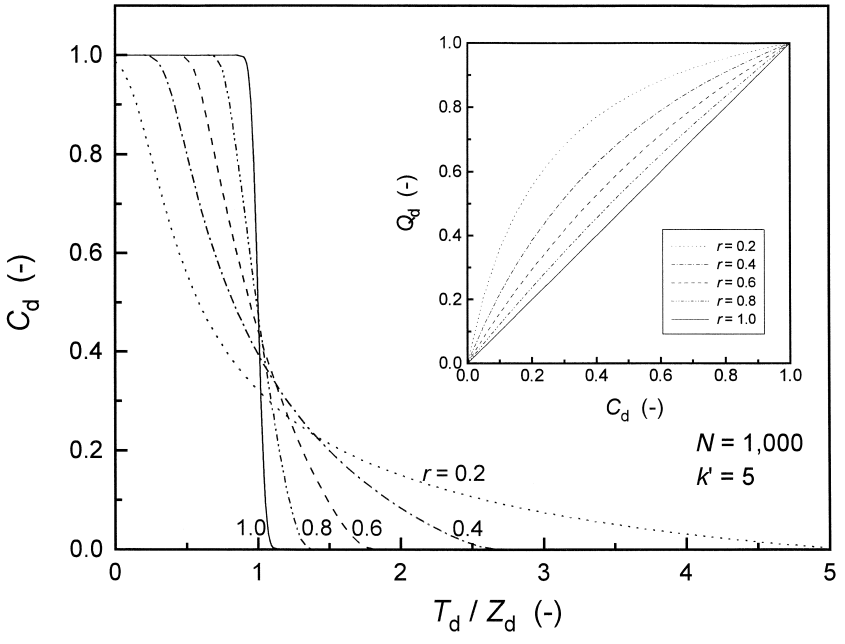

Fig. 1. Influence of the change in r on the diffuse profile of rear boundary curves. Inset: the profiles of original (true) Langmuir isotherms. Note that the symbol (–) used in all figures means that the parameter is dimensionless.

equilibrium with C. The overall mass transfer resistance in the column is accounted for by two kinetic parameters, i.e., D_L and k_m. The contributions of all the mass transfer processes in the column to peak broadening, except for that of axial dispersion, i.e., fluid-to-particle mass transfer, intraparticle diffusion, and adsorption/desorption kinetics are lumped into one rate coefficient, k_m.

In the equilibrium-dispersive model [1], the individual contributions of all the mass transfer processes in the column to band broadening are lumped into a single kinetic parameter, D_a, and in Eq. (13), D_L is replaced by D_a. It is also assumed that the mass transfer rate between the stationary and mobile phases is large enough to allow considering the rate coefficient, k_m, as infinite. The height equivalent to a theoretical plate (HETP) calculated in the equilibrium-dispersive model (H_{Pe}) is correlated with D_a as follows

$$H_{Pe} = \frac{2L}{Pe_L} = \frac{2D_a}{u} \tag{15}$$

Similarly, in the transport model [1], it is assumed that $D_L = 0$ in Eq. (13) and the contribution of axial dispersion is lumped with those of mass transfer kinetics. In this case, the individual contributions of all the mass transfer processes in the column to band broadening are accounted for by the lumped mass transfer rate coefficient ($k_{m,L}$). The HETP in the transport model (H_{St}) is correlated with the Stanton number (St) as follows

$$H_{St} = \frac{K}{(1+K)^2} \cdot \frac{2L}{St} \tag{16}$$

with

$$St = \frac{k_{m,L}L}{u} \tag{16a}$$

where K is the partition coefficient in nonlinear chromatography [$=F(\partial q/\partial C)$].

Fig. 2 shows the elution profiles of the overloaded peaks at different L_f values calculated by the equilibrium-dispersive model under a series of hypothetical conditions, which are also listed in Fig. 2. In this case, the overall mass transfer resistance is due to axial dispersion. The contribution of the mass transfer kinetics to peak broadening is negligibly small.

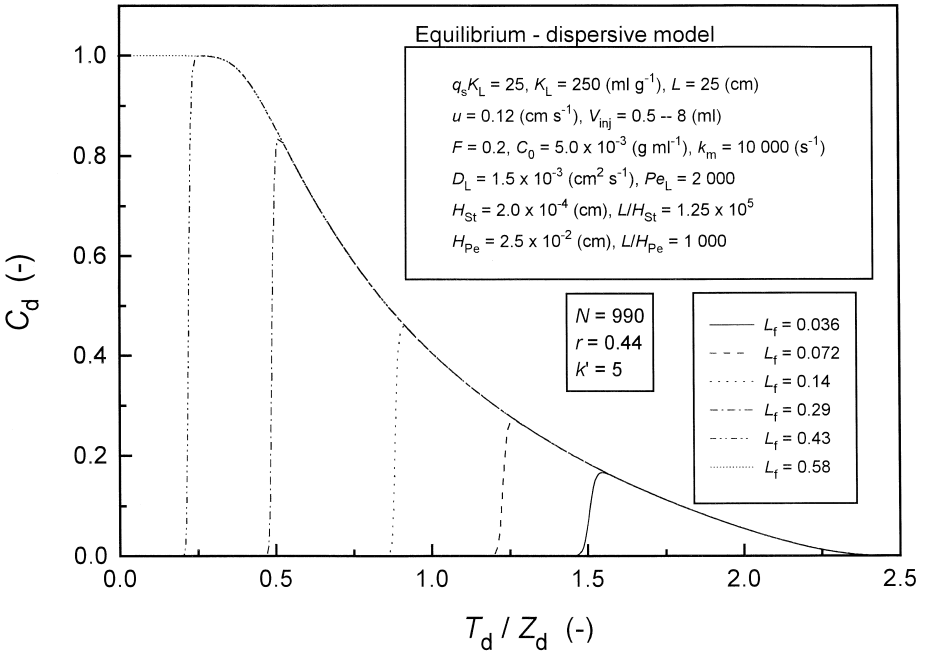

Fig. 2. Elution peak profiles calculated for different L_f values by the equilibrium-dispersive model.

The three dimensionless parameters other than L_f are $N=990$, $r=0.44$, and $k'=5$. Note that the diffuse profiles of all the overloaded peaks agree well together and with the rear boundary of the desorption curve even though the column efficiency is not high, $N\approx1000$. The desorption profile is also consistent with the results in Fig. 1.

Fig. 3 shows similar peak profiles at different L_f values calculated by the transport model under nearly equivalent hypothetical conditions. The contribution of the mass transfer kinetics to peak broadening is tentimes larger than the contribution of axial dispersion. The diffuse profiles of all the overloaded peaks and the rear boundary of the desorption curve in Fig. 3 are superimposed with those in Fig. 2 (the column efficiencies are nearly identical). We also confirmed that the same profiles were obtained for overloaded peaks and for the desorption curve for different combinations of the contributions of axial dispersion and the mass transfer kinetics but at constant overall column efficiency (not shown). These results allow the conclusion that the results of this study, although derived from calculations based on the equilibrium-dispersive model, can be used for the analysis and the correction of the influence of the mass transfer resistances on the determination of the equilibrium isotherm by the ECP method, irrespective of the relative contribution of axial dispersion and the mass transfer kinetics to band broadening.

3. Experimental

3.1. Chemicals

A chiral stationary phase, Chiracel OB, which is a cellulose tribenzoate coated on a silica gel substrate, 20 μm particles (Daicel, Tokyo, Japan) was used. The stationary phase was a gift from Chiral Technologies (Exton, PA, USA). HPLC grade *n*-hexane and ethyl acetate were purchased from Fisher Scientific (Fair Lawn, NJ, USA). The sample compounds, *S*-1-phenyl-1-propanol (*S*-PP) and *R*-1-phenyl-1-propanol (*R*-PP), and an inert tracer, 1,3,5-tri-*tert*.-butylbenzene, were obtained from Aldrich (Milwaukee, WI, USA). Although both PP enantiomers were more than 99% pure, the products received from the manufacturer contained an impurity that absorbed significantly at the best wavelength for detection and needed to be removed. The detailed

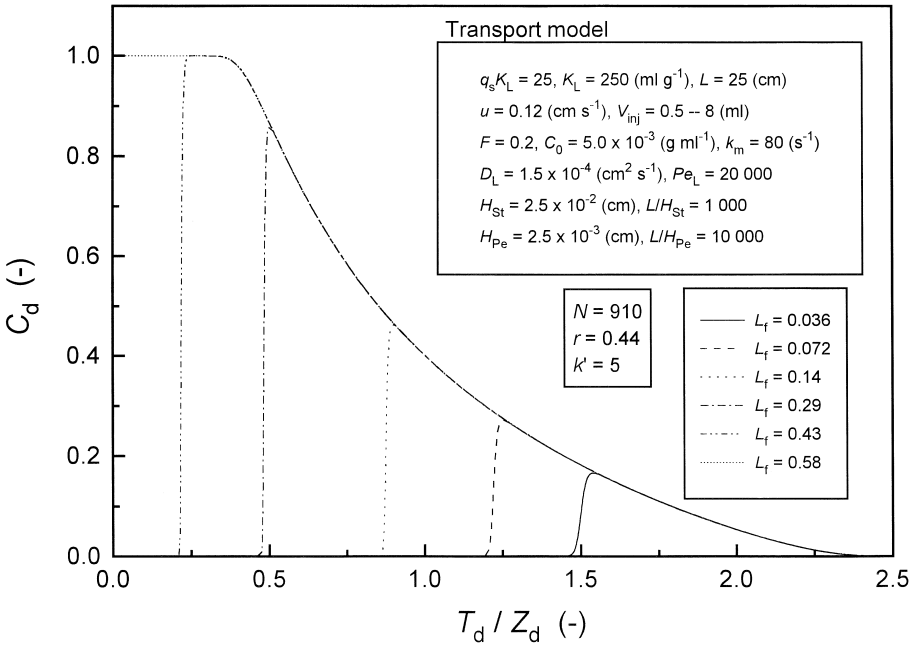

Fig. 3. Elution peak profiles calculated for different L_f values by the transport-dispersive model.

information about the purification of the enantiomers was described previously [11].

3.2. Equipment

All the experiments made for the determination of the equilibrium isotherm and the measurement of overloaded elution peaks were carried out with an HP 1090 liquid chromatograph (Hewlett-Packard, Palo Alto, CA, USA), equipped with a ternary-solvent delivery system, an automatic sample injector with a 250 μl loop, a diode-array UV detector, and a computer data acquisition system using the HP-ChemStation software (version A.05.03). The acquired data were downloaded to one of the computers at The University of Tennessee Computer Center for further data processing.

3.3. Chromatographic conditions

In all the experiments, we used a 20×1.0 cm I.D. column, packed in-house with the chiral stationary phase, Chiracel OB. The mobile phase was a mixture of *n*-hexane–ethyl acetate (95:5, v/v). The volumetric flow-rate of the mobile phase was 2.5 ml min^{-1}. The total porosity of the column ($\varepsilon = 0.721$) was determined by injecting a nonretained compound, 1,3,5-tri-*tert*.-butylbenzene. The efficiency of the column (N = ca. 1000 plates) was determined from the width of the peak at half height. All experiments were performed at room temperature (22–24°C).

3.4. Procedures

The single component adsorption isotherms of both PP enantiomers were measured using single-step FA. Sample solutions at different concentrations of each solute were prepared by successively mixing the pure mobile phase with a high concentration solution (5.60 g l^{-1} for *S*-PP and 5.43 g l^{-1} for *R*-PP). The concentration step used in FA was 5 or 10% of the concentration of this second solution. The injection of a large volume (ca. 15 ml) of the sample solution resulted in the elution of a breakthrough curve followed by a concentration plateau. The amount of the enantiomer adsorbed by the chiral stationary phase at equilibrium was determined from the elution time of the inflection point of this breakthrough curve. The UV detector was calibrated at 270 nm, using the concentration plateaus in order to relate the UV-absorbance and the solute concentrations. The experimental data were fitted to the Langmuir model. Other sample solutions, of higher concentration (9.15 g l^{-1} for *S*-PP and 7.76 g l^{-1} for *R*-PP), were used for the acquisition of the profiles of strongly overloaded elution peaks. The injection volumes were 0.25, 1.0, and 2.0 ml.

4. Results and discussion

We first studied successively the influence of each of the four parameters on the error of measurement made on the parameters of a single component isotherm by ECP. Then, the concentration range of the objective isotherm accessible by ECP was investigated. Finally, an attempt was made experimentally to demonstrate the effectiveness of the results of the nondimensional numerical calculations.

4.1. Influence of L_f

Fig. 4 shows the elution profiles of overloaded peaks at various L_f values. The other three parameters are $N = 1000$, $r = 0.5$, and $k' = 5$. The dimensionless concentration at the apex ($C_{d,ap}$) increases with increasing L_f. The value of $C_{d,ap}$ is almost equal to unity at $L_f = 0.3$. As shown in Fig. 2, the diffuse profiles of all the overloaded peaks agree well together and with the rear boundary of the desorption curve, even for an efficiency of only $N = 1000$.

The isotherms derived from the elution peak profiles in Fig. 4 by applying the ECP method (lines) are compared with the original (true) Langmuir isotherm (open circles) in Fig. 5. The arrows in the figure show $C_{d,ap}$ at different L_f values. When L_f is smaller than about 0.3, the whole arc (0–C_o) of the objective isotherm cannot be determined. However, the arcs of isotherm estimated by ECP from each elution peak in Fig. 4 are well superimposed, irrespective of L_f. The slight discrepancy observed between the estimated isotherms and the true Langmuir isotherm is due to the finite column efficiency, $N = 1000$.

The values measured by ECP for the amount

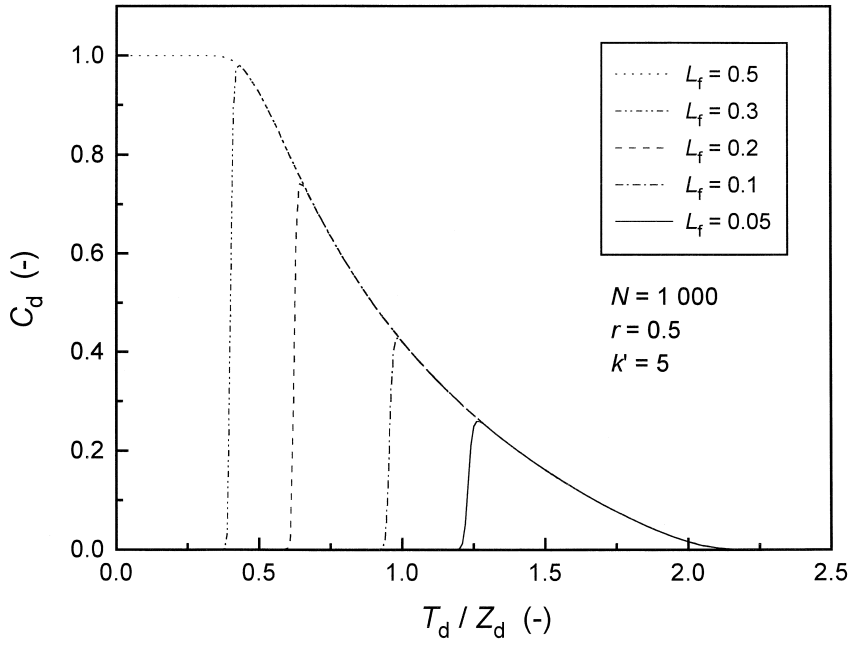

Fig. 4. Elution peak profiles for different L_f values.

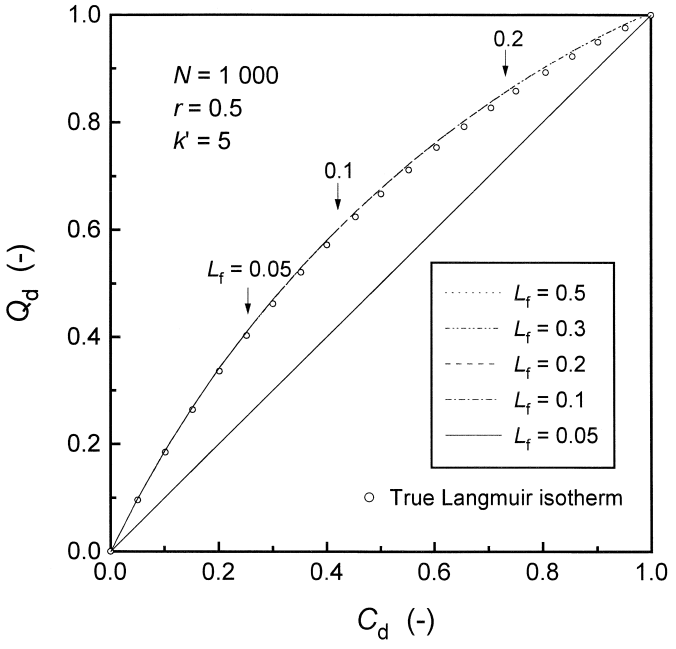

Fig. 5. Comparison of the isotherms measured by the ECP method for different L_f values with the original (true) Langmuir isotherm. The arrows indicate $C_{d,ap}$ at different L_f values.

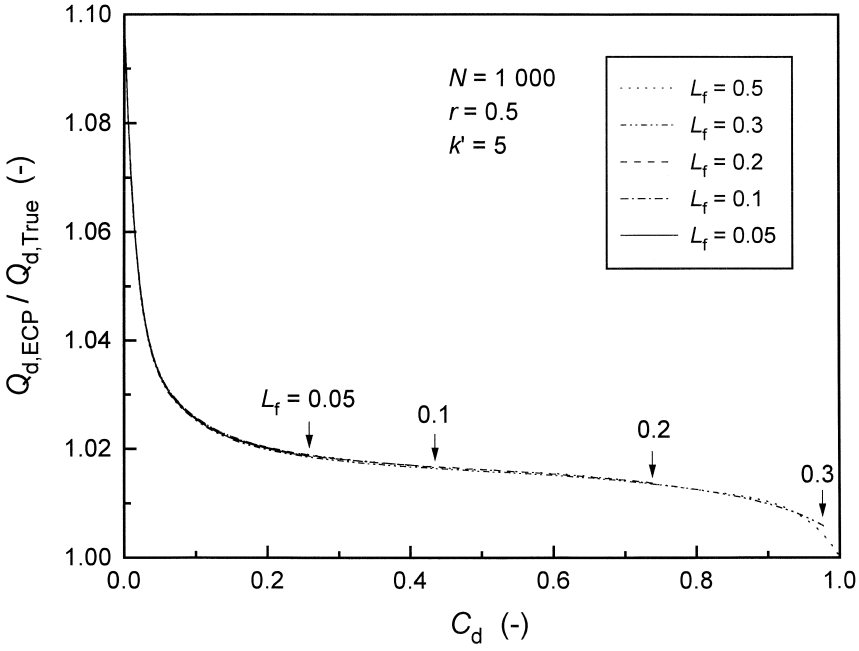

Fig. 6. Accuracy of the ECP method as a function of C_d at different L_f values. The arrows indicate $C_{d,ap}$ at different L_f values.

adsorbed ($Q_{d,ECP}$) at a given C_d are compared with the ideal ones ($Q_{d,True}$) in Fig. 6. The ratio $Q_{d,ECP}/Q_{d,True}$ decreases with increasing C_d, and reaches unity at $C_d = 1.0$. As illustrated in Figs. 5 and 6, only part of the isotherm can be determined when L_f is lower than about 0.3 under the conditions described above. As in Fig. 5, the arrows in Fig. 6 indicate $C_{d,ap}$ at different L_f values. However, the isotherms estimated by the ECP method at different L_f values are in excellent agreement with each other. In the following discussion, we took $L_f = 0.2$, which corresponds to a strong degree of column overloading.

4.2. Influence of r

This parameter characterizes the curvature of the isotherm in the concentration range investigated. Note that, for various reasons (e.g., solubility), it is exceptional to carry out measurements with $K_L C_0 > 1$, i.e., $r < 0.5$. Fig. 7 shows elution peak profiles obtained for different values. As shown in Fig. 1, the degree of band tailing becomes important when r decreases. Increasing band broadening and tailing are accompanied with a decrease of the peak height (Fig. 7). The apparent peak area increases with increasing r even though L_f is constant at 0.2 because $T_{d,p}$ is related with r (Eq. (10)) and the time scale changes with r. The value of $C_{d,ap}$ is almost equal to unity at $r = 0.6$ under the selected conditions ($N = 1000$, $k' = 5$, and $L_f = 0.2$).

Fig. 8 compares the isotherms derived by ECP (solid line) and the true Langmuir one (dotted line) at different values of r. The correlation between $Q_{d,ECP}/Q_{d,True}$ and C_d calculated from the data in Fig. 8 is given in Fig. 9. The error made in the determination of the objective isotherm at low concentrations increases with increasing r. However, when r is small, the objective isotherm can be determined only in a narrow concentration range because L_f is kept constant. At high concentrations, the profiles of the curves in Fig. 9 are independent of r.

4.3. Influence of N

Fig. 10 represents the influence of N on the profile of overloaded elution peaks ($r = 0.5$, $k' = 5$, and $L_f = 0.2$). As expected, the profiles become steeper as N increases. However, the difference in peak height

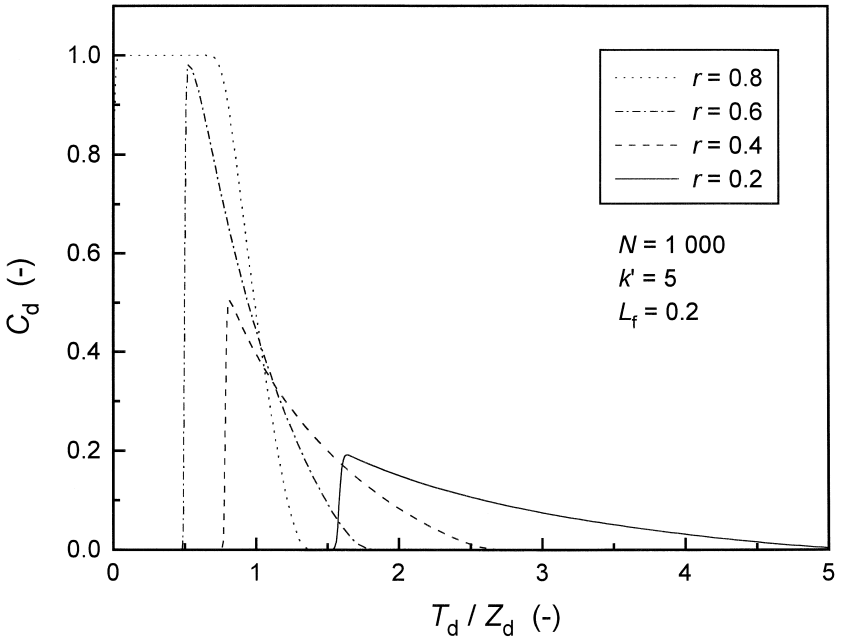

Fig. 7. Elution peak profiles at different r values.

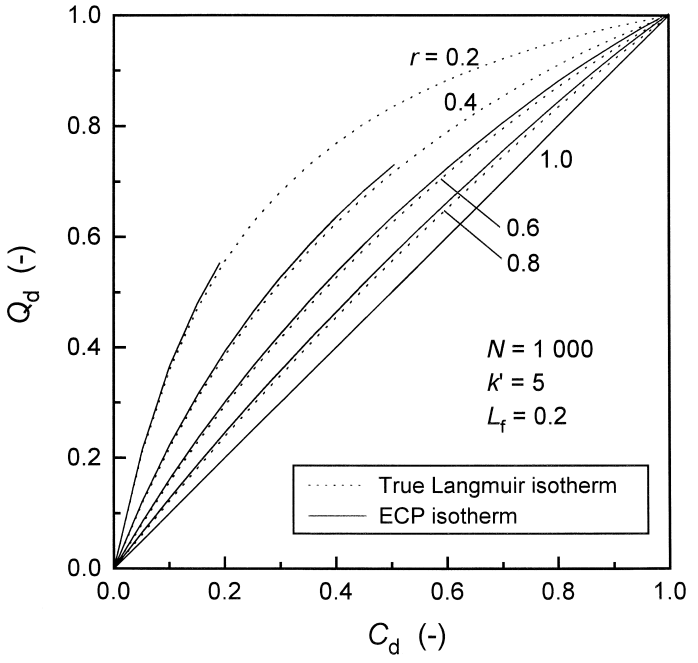

Fig. 8. Comparison of the isotherms estimated by the ECP method at different r values with the original (true) Langmuir isotherms.

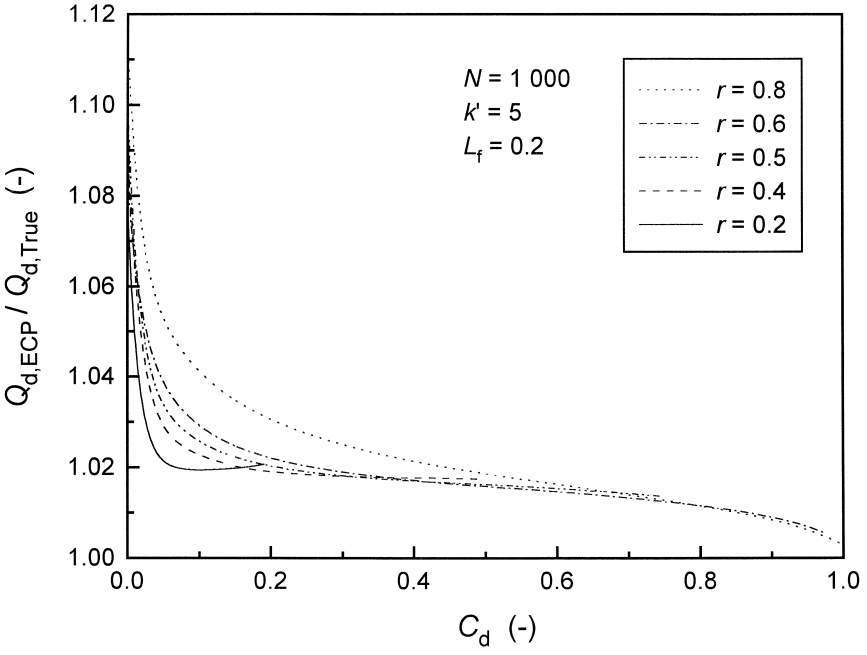

Fig. 9. Accuracy of the ECP method as a function of C_d at different r values.

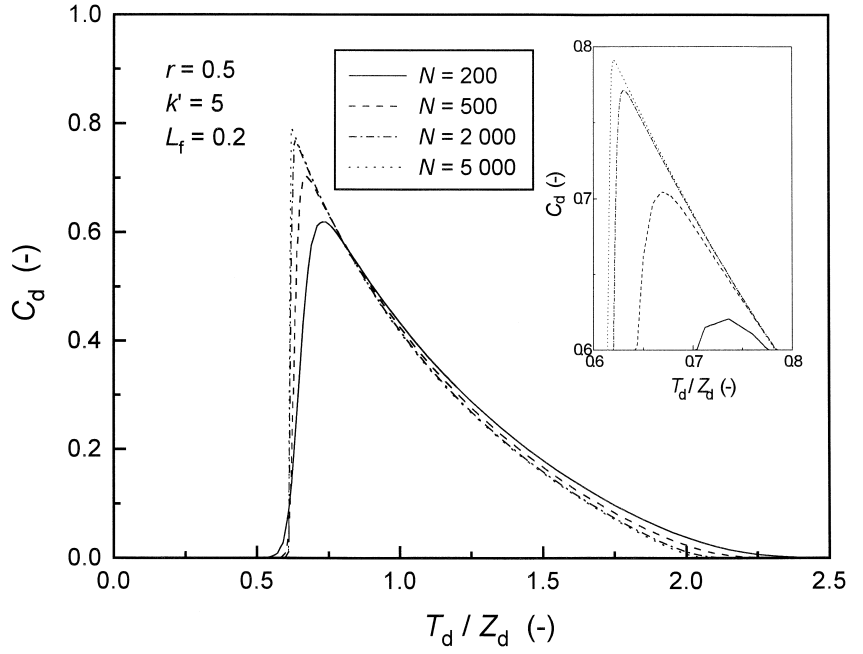

Fig. 10. Elution peak profiles at different N values. Inset: enlargement of the area around the top of the peak profiles.

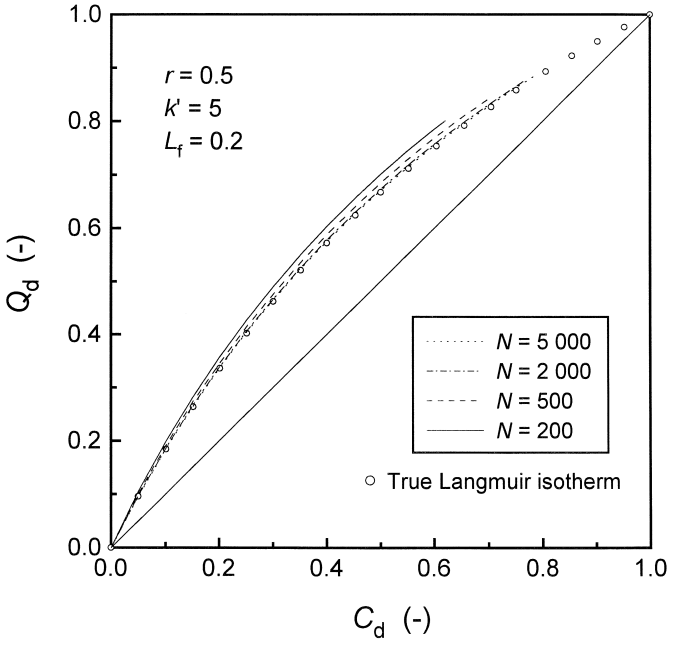

Fig. 11. Comparison of the isotherms estimated by the ECP method at different N values with the original (true) Langmuir isotherm.

($C_{d,ap}$) at $N=5000$ and 500 is only about 0.1, in spite of the large difference in column efficiencies.

Fig. 11 compares the isotherms derived by ECP at different plate numbers and the true Langmuir isotherm. The discrepancy increases with decreasing column efficiency [10]. In Fig. 12, the ratio $Q_{d,ECP}/Q_{d,True}$ is plotted against C_d. For N between 500 and 5000, the concentration range within which the objective isotherm can be assessed by ECP remains nearly constant, $C_{d,ap}=0.7–0.8$. However, the error is important and decreases rapidly with increasing column efficiency. Although the error may exceed 10% at very low concentrations, the data points of the isotherm can be determined with a relative error less than 1% when N is larger than 2000. These results are consistent with the conclusions of the study of the accuracy and precision of the ECP method reported by Guan et al. [10].

When a compound is very expensive (e.g., pharmaceuticals and biologically active substances), its isotherm must be determined by using as small an amount as possible. Then, a relatively small column must be used in order to avoid wasting the compound while keeping L_f high. However, reducing the column length brings about a reduction in N and a larger error caused by ECP. Jacobson et al. [9] claimed that no corrections could be made to account for band spreading due to mass transfer resistances in the column in FACP and ECP and that this is the main potential drawback of these methods. Even under such conditions, however, the results in Fig. 12 suggest that the error caused by the mass transfer resistance in the measurement of equilibrium data by ECP could be corrected. A similar correlation can be made for FACP, using the results of numerical calculations made in the assumption of a large enough value of L_f.

Results provided by nondimensional numerical calculations could be effective for improving the accuracy of the determination of the objective isotherm by ECP and FACP. A correction procedure of experimental data acquired with insufficiently efficient columns could be useful for extending the possibilities of ECP and FACP to rare and expensive chemicals. Later in this study, we develop a correction procedure based on the results shown in this section and attempt to give an experimental demonstration of its usefulness.

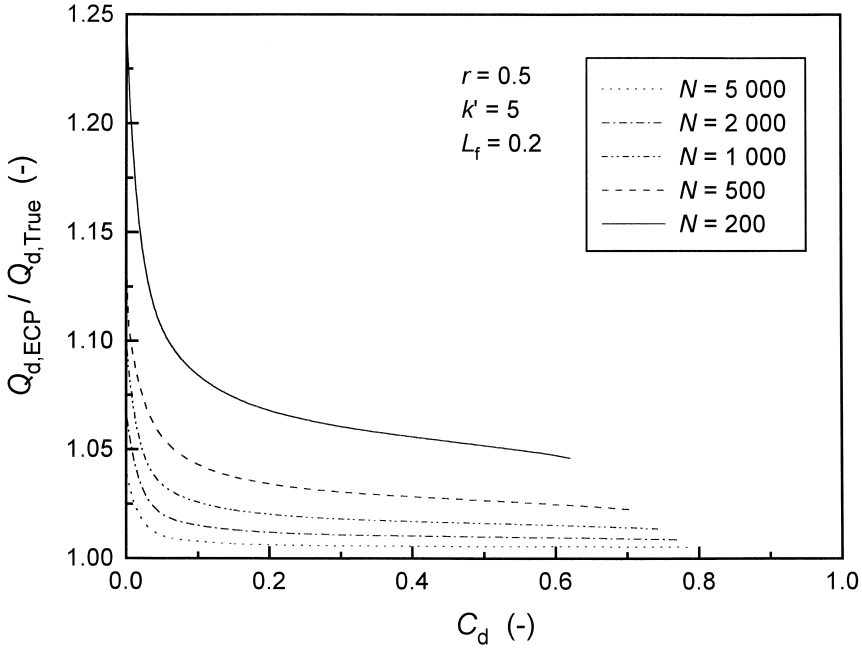

Fig. 12. Accuracy of the ECP method as a function of C_d at different N values.

4.4. Influence of k'

Fig. 13 illustrates the influence of k' on overloaded peak profiles (N, r, and L_f are taken as 1000, 0.5, and 0.2, respectively). The steepness of the profile increases slightly with increasing k'. The differences in $C_{d,ap}$ at various k' values are small. The evaluation of the influence of k' on the elution behavior cannot be made easily by an experimental approach because chromatographic processes are affected by various factors. For example, the retention factor can be changed by adjusting the mobile phase composition, i.e., the nature and concentration of the organic modifier in RPLC. However, the influence of the mobile phase composition on the retention is most complicated. A change in the mobile phase composition is followed by changes in the parameters of the isotherm and of the mass transfer processes. Then, the values of all four parameters change simultaneously.

Fig. 14 shows the isotherms derived by ECP at various k' values and the original (true) Langmuir isotherm. The discrepancy between the measured and the true isotherm decreases with increasing k'. The error caused by ECP is illustrated in Fig. 15 as a function of C_d. It is quite significant, in part because of the relatively low column efficiency ($N=1000$). However, the correlations between $Q_{d,ECP}/Q_{d,True}$ and C_d are almost identical for $k'>5$.

4.5. Concrete instance of the application of the numerical calculation results to the estimation of the equilibrium isotherm by the ECP method

The results of the nondimensional numerical calculations described earlier show that the error made in determining equilibrium isotherms by ECP are most important under the following conditions: (1) if the radius of curvature of the Langmuir isotherm is small (i.e., if r is large); (2) if the column efficiency is low; and (3) if the retention of the solute is small (i.e., if k' is small). A change in loading factor, L_f, has no influence on the error made on the isotherm by ECP. Only the concentration range within which the equilibrium isotherm is accessible by ECP varies with L_f. These results suggest also that the error made on the isotherm by

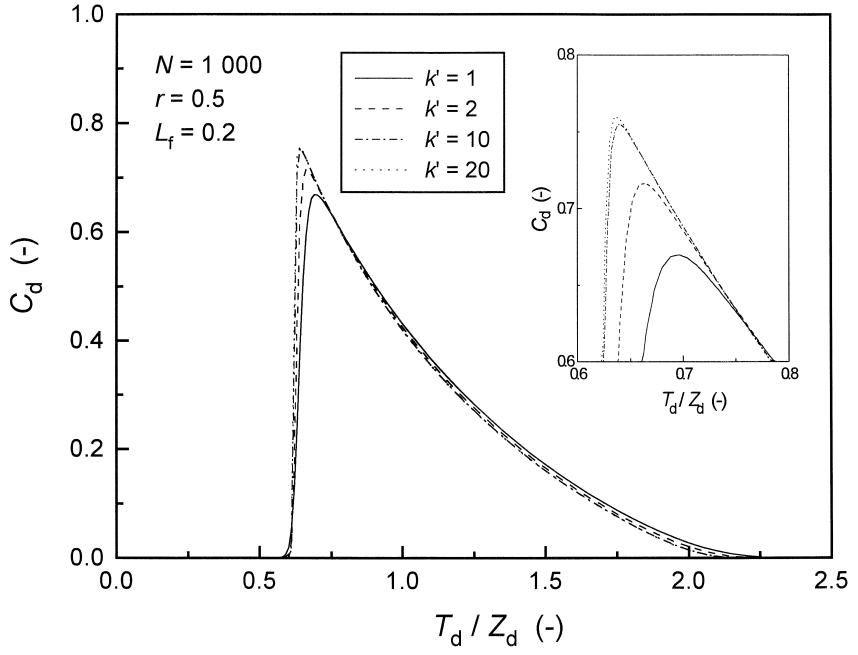

Fig. 13. Elution peak profiles at different k' values. Inset: enlargement of the area around the top of the peak profiles.

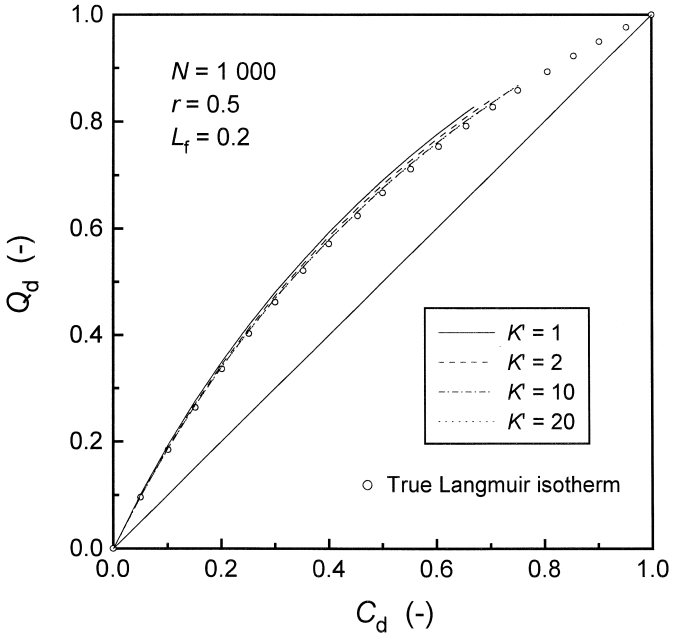

Fig. 14. Comparison of the isotherms estimated by the ECP method at different k' values with the original (true) Langmuir isotherm.

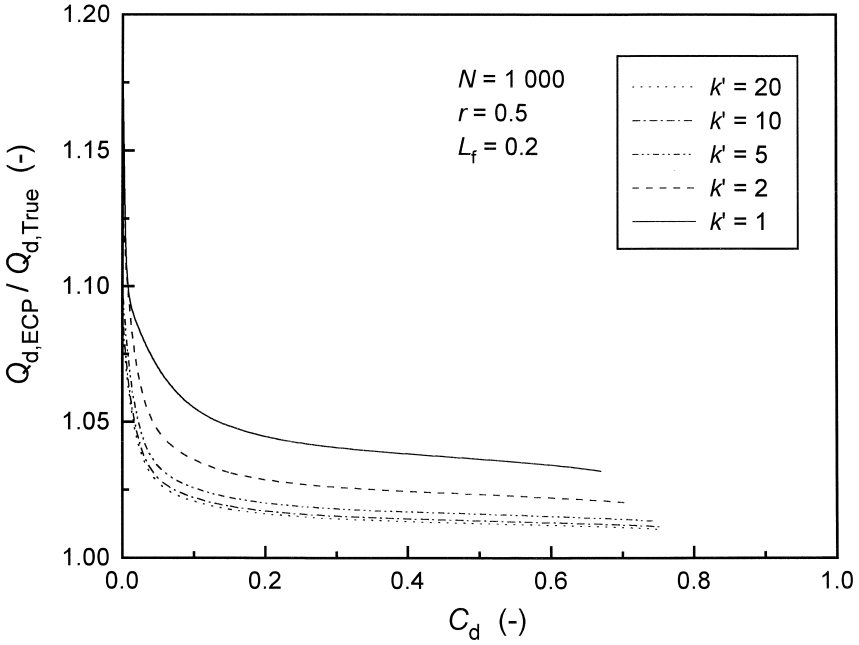

Fig. 15. Accuracy of the ECP method as a function of C_d at different k' values.

ECP could be corrected by applying a numerical correction.

In this section, we attempt to demonstrate the usefulness of the numerical calculation for improving the accuracy of the determination of isotherms by ECP. To this purpose, we used a system previously studied in this group, the enantiomeric separation of *R*-PP and *S*-PP on the chiral stationary phase Chiracel OB, with *n*-hexane–ethyl acetate (95:5, v/v) as the mobile phase. In this system, the values of the four chromatographic parameters for *R*-PP were $N=1000$, $r=0.54$, $k'=1.6$, $L_f=0.046$ and 0.092. The two parameters r and L_f were calculated from the equilibrium isotherm measured by the FA method. Under these conditions, ECP cannot provide sufficiently accurate data and FA was used to determine the single component isotherms [11]. These FA data are thus available to compare with those obtained directly by ECP and with those obtained by a suitable correction of the ECP data.

Fig. 16 shows the experimental data for the phase equilibrium of *R*-PP (open circle), which were determined by FA. The dotted line shows the best fit Langmuir isotherm of these experimental equilibrium data. The corresponding Langmuir parameters are listed in Table 1. Fig. 16 also shows the equilibrium isotherm (dashed line) calculated by ECP from the rear diffuse profile of the overloaded elution band at $L_f=0.092$. Although the equilibrium isotherm can be determined in the range $0<Q_d<$ ca. 0.6, a significant discrepancy is observed between the dotted and dashed lines, as expected given the low column efficiency. Table 1 also lists the Langmuir parameters of the equilibrium isotherm estimated by ECP (dashed line in Fig. 16). The model error made on the equilibrium isotherm by ECP is plotted in Fig. 17 versus C_d (dashed line at $L_f=0.092$). The ratio of $Q_{d,ECP}$ to $Q_{d,True}$ ranges between ca. 1.07 and 1.11.

Similar to those shown in Figs. 6, 9, 12 and 15, the correlation between the ratio $Q_{d,ECP}/Q_{d,True}$ and C_d was calculated in this concrete case (Fig. 18). The curve in Fig. 18 is located between the same correlations calculated for $k'=1$ and 2 and reported in Fig. 15. It was attempted to correct the model error in Fig. 16 by using the numerical correlation calculated between $Q_{d,ECP}/Q_{d,True}$ and C_d in Fig. 18 as a correction. The result of this exercise was the corrected isotherm (solid line) shown in Fig. 16. Although a certain discrepancy is still observed between the isotherm determined by the FA (dotted

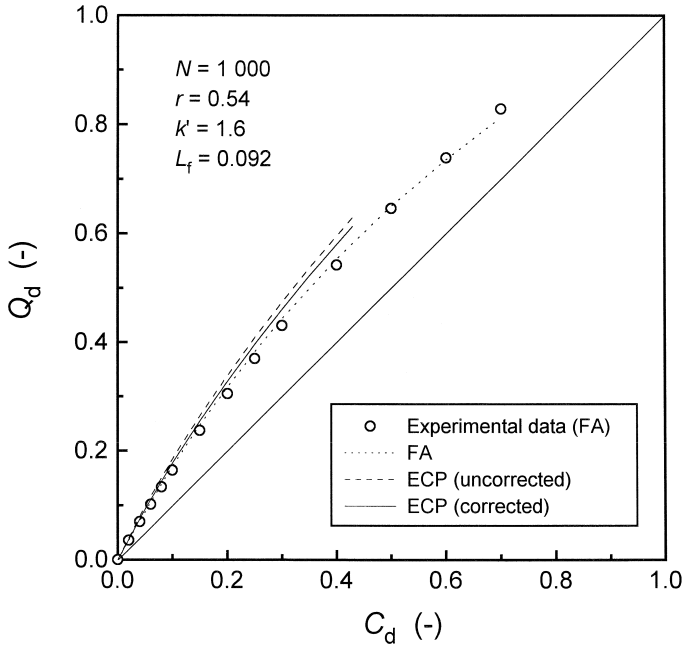

Fig. 16. Comparison of the isotherms of *R*-PP estimated by the ECP method with that determined by the FA method.

line) and the one estimated by the ECP method and corrected as just explained (solid line), the magnitude of this discrepancy decreased by half. As shown by the solid line at $L_f = 0.092$ in Fig. 17, the error made on the equilibrium isotherm by the ECP method is reduced by one-half. The two Langmuir parameters, q_s and K_L, of the corrected isotherm (solid line in Fig. 16) are listed in Table 1. They are closer to those derived by FA than those obtained from the uncorrected data (dashed line in Fig. 16). The error in the estimation of the Langmuir parameters is larger at $L_f = 0.046$ than at 0.092 because a more limited range of the equilibrium isotherm is assessed at $L_f = 0.046$. However, almost the same situation is observed for the correlation between $Q_{d,ECP}/Q_{d,True}$ and C_d at $L_f = 0.046$ (solid and dashed lines) in Fig. 17. In conclusion the error made in determining the equilibrium isotherm by ECP and caused by band spreading can be corrected by applying the results of the numerical calculation.

When a high efficiency column (e.g., with $N >$ 2000) is used, the objective isotherm can be determined with a reasonable accuracy by the ECP method [10]. On the other hand, when the column has a moderate or low efficiency, e.g., 1000 plates or fewer, a correction should be made to the isotherm

Table 1
Parameters of the Langmuir isotherms of *R*-PP determined by the FA and ECP methods

	FA	ECP			
		Injection volume 1.0 ml		Injection volume 2.0	
		Uncorrected	Corrected	Uncorrected	Corrected
q_s (g l^{-1})	38.5	29.4	32.3	34.3	36.9
K_L (l g^{-1})	0.11	0.16	0.14	0.14	0.12
$q_s K_L$ (–)	4.2	4.8	4.5	4.7	4.5

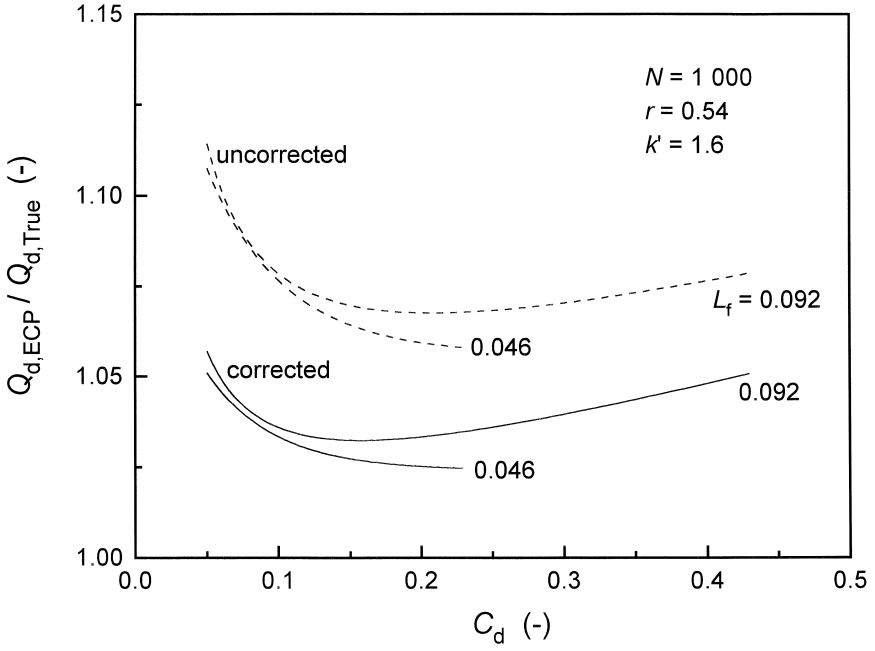

Fig. 17. Correlation between $Q_{d,ECP}/Q_{d,True}$ and C_d for the corrected and uncorrected isotherms of *R*-PP.

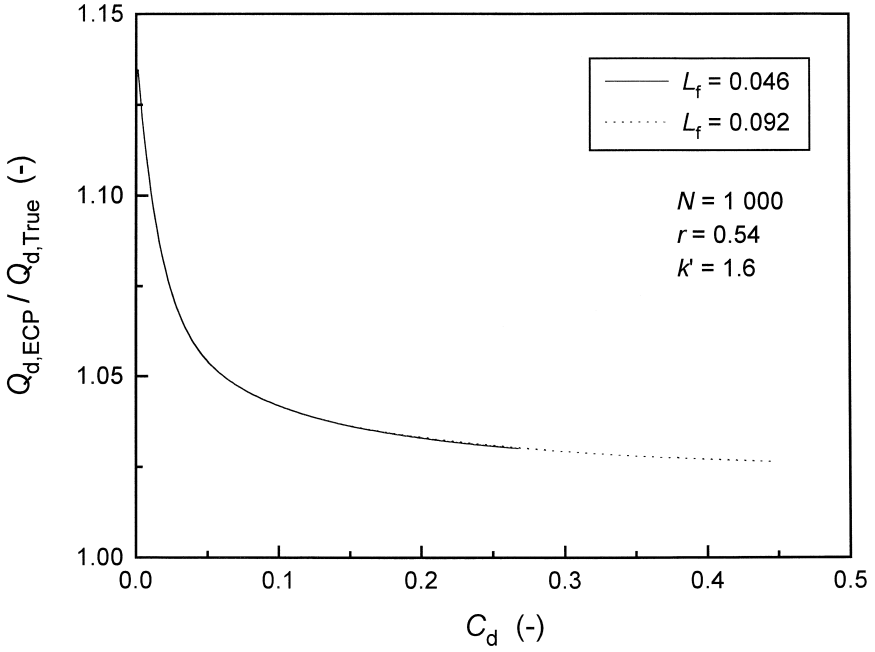

Fig. 18. Accuracy of the ECP method as a function of C_d at the experimental conditions, i.e., $N=1000$, $r=0.54$, and $k'=1.6$.

measured by the ECP method. In this case, an apparent isotherm is first calculated from the rear diffuse profile of an overloaded elution peak, using the conventional ECP method. Then, the two parameters r and L_f are estimated from the apparent isotherm. The other two parameters (N and k') are derived from a chromatogram obtained under linear conditions, with a small sample. Finally, the apparent isotherm is corrected on the basis of the results of the numerical calculations reported earlier, using these four parameters. Figs. 11 and 12 show that the apparent isotherm is not very different from the objective isotherm. However, the error made in estimating the objective isotherm in this manner increases with decreasing column efficiency. Further work is needed to elucidate the relationship between the residual error after this correction and the column efficiency.

4.6. Concentration range of equilibrium isotherm

Fig. 19 shows the correlation between $C_{d,ap}$ and L_f for $N=1000$ and $k'=5$. The value of $C_{d,ap}$ depends also on these experimental conditions. The larger the value of r, the steeper the initial slope or $\partial C_{d,ap}/\partial L_f$. When $r=0.8$, $C_{d,ap}$ is close to unity, even at $L_f=0.1$. By contrast, the rate of increase of $C_{d,ap}$ is small at high curvature of the objective isotherm. The value of $C_{d,ap}$ reaches only 0.55 at $r=0.2$, even when a very large sample is injected, i.e., at $L_f=0.5$. As shown in Figs. 10 and 13, the influence of N and k' on the apical height of overloaded elution peaks is small. The results in Fig. 19 can be used as a basis for the estimation of $C_{d,ap}$ in ECP under standard chromatographic conditions. In order to demonstrate the validity of the curves, several sets of experimental data obtained in this study and in a previous paper [12] are also plotted in Fig. 19. The information on the nondimensional parameters, N, r, k', and L_f, is listed in Table 2. Although k' does not vary in a wide range, the points corresponding to most experimental data are close to the lines in Fig. 19. The experimental conditions, including L_f, must be chosen according to the intended concentration range

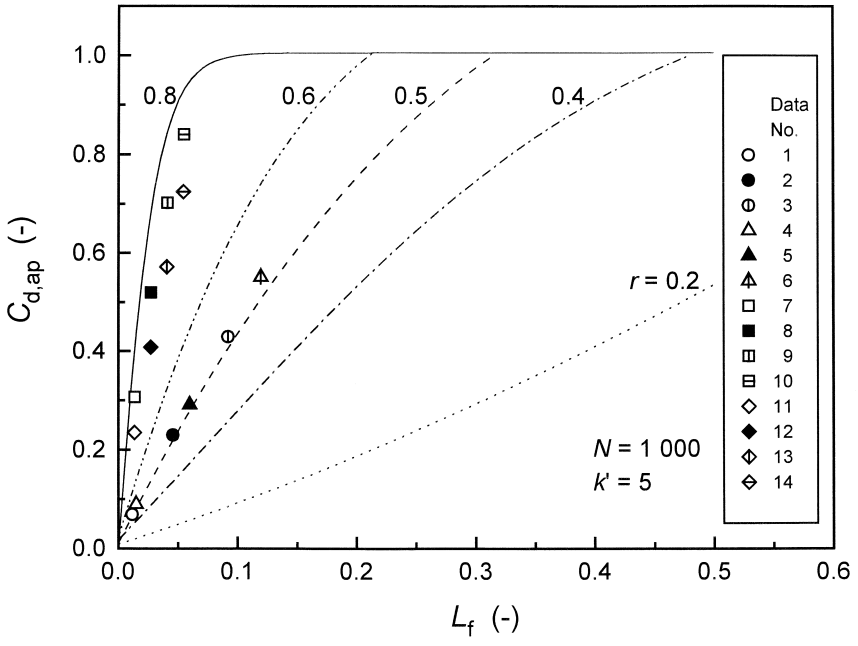

Fig. 19. Correlation of $C_{d,ap}$ with L_f. Symbols show experimental data. Data number refers to Table 2. Lines indicate the results of the numerical calculations at $N=1000$ and $k'=5$.

Table 2
Experimental conditions

Solute	Stationary phase	Mobile phase	N	r	k'	L_f	Data number	Ref.
R-PP	Chiracel OB	*n*-Hexane–ethyl acetate (95:5, v/v)	1000	0.54	1.6	0.011	1	This work
						0.046	2	This work
						0.092	3	This work
S-PP	Chiracel OB	*n*-Hexane–ethyl acetate (95:5, v/v)	1000	0.55	1.2	0.015	4	This work
						0.060	5	This work
						0.12	6	This work
R-3-Cl-PP[a]	Chiracel OB-H	*n*-Hexane–ethyl acetate (95:5, v/v)	8000	0.73	2.5	0.014	7	[12]
						0.027	8	[12]
						0.041	9	[12]
						0.054	10	[12]
S-3-Cl-PP[b]	Chiracel OB-H	*n*-Hexane–ethyl acetate (95:5, v/v)	8200	0.76	2.1	0.014	11	[12]
						0.028	12	[12]
						0.041	13	[12]
						0.055	14	[12]

[a] *R*-3-chloro-1-phenyl-1-propanol.
[b] *S*-3-chloro-1-phenyl-1-propanol.

of the objective isotherm. The results in Fig. 19 demonstrate that numerical calculations are also useful for this purpose.

5. Conclusion

The use of a nondimensional model and numerical calculations allow the determination of the accuracy of single component isotherms measured by ECP. The influence of the four parameters, N, r, k', and L_f, involved in the nondimensional equations, on the systematic error made on the objective isotherm could be assessed. As shown in Figs. 6, 9, 12 and 15, the influence of each parameter on the error made in the determination of the equilibrium isotherm by ECP depends on the other experimental conditions. For instance, the profiles of the correlations between $Q_{d,ECP}/Q_{d,True}$ and C_d are almost independent of L_f. When L_f is varied, only $C_{d,ap}$ changes, not the error (Fig. 6). The error curves at different r values agree closely at high concentrations (Fig. 9). Unfortunately, ECP must use the low concentration data where the errors are more important. The degree of non-equilibrium in chromatography is obviously larger for low efficiency than for high efficiency columns (Fig. 12). Finally, when $k'>5$, changes in k' hardly influence the accuracy of isotherm measurements. In conclusion, the correlation between $Q_{d,ECP}/Q_{d,True}$ and C_d depends only on r and N for k' larger than 5 (Fig. 15).

Correlations between $Q_{d,ECP}/Q_{d,True}$ and C_d can be calculated numerically under given sets of experimental conditions using nondimensional basic equations. In principle, the influence of the finite column efficiency on the accuracy of equilibrium data measurements by ECP can be corrected using the correlation curve between $Q_{d,ECP}/Q_{d,True}$ and C_d. This would allow an extension of the applicability of ECP and FACP. These methods could be used with short columns having a low efficiency to prevent waste of time, chemicals and solvents. The concentration range within which the objective isotherm must be determined depends on the experimental conditions. The necessary amount of compound can be determined from the peak heights, also estimated by nondimensional calculations. Application of the corrections derived from the numerical calculations discussed to experimental data proved effective in reducing the errors made on the isotherms derived by ECP. The excellent agreement between the diffuse boundaries of the profiles of the overloaded peaks

calculated by the equilibrium-dispersive and the transport models suggests that the numerical results of this study, although mostly based on the equilibrium-dispersive model, are also probably applicable to peak broadening phenomena arising from a slow mass transfer kinetics.

6. List of symbols

C	Actual concentration
C_d	Dimensionless concentration
$C_{d,ap}$	Dimensionless apical concentration
C_i	Actual concentration at V_i
C_0	Actual concentration of the feed solution
D_a	Apparent axial dispersion coefficient
D_L	Axial dispersion coefficient
F	Phase ratio $(=(1-\epsilon)/\epsilon)$
H_{Pe}	Height equivalent to a theoretical plate calculated from D_a
H_{St}	Height equivalent to a theoretical plate calculated from $k_{m,L}$
k_m	Mass transfer rate coefficient representing the contributions of the fluid-to-particle mass transfer, the intraparticle diffusion, and the adsorption/desorption to band broadening
$k_{m,L}$	Lumped mass transfer rate coefficient representing the contributions of the axial dispersion, the fluid-to-particle mass transfer, the intraparticle diffusion, and the adsorption/desorption to band broadening
k'	Retention factor
K	Partition coefficient in nonlinear chromatography $[=F(\partial q/\partial C)]$
K_L	Langmuir parameter
L	Column length
L_f	Loading factor
n	Amount of solute injected
N	Number of theoretical plates
Pe_L	Column Peclet number
q	Actual amount adsorbed
q_i	Actual amount adsorbed in equilibrium with C_i
q_s	Saturation capacity
q_0	Actual amount adsorbed in equilibrium with C_0, calculated with Eq. (3)
q^*	q In equilibrium with C
$\partial q/\partial C$	Slope of the isotherm chord
Q_d	Dimensionless amount adsorbed
$Q_{d,ECP}$	Dimensionless amount adsorbed estimated by the ECP method
$Q_{d,True}$	Dimensionless amount adsorbed in equilibrium with C_d
r	Dimensionless Langmuir equilibrium constant, defined in Eq. (5)
S	Column cross-sectional area
St	Stanton number
t	Actual time
T_d	Dimensionless time
$T_{d,p}$	Dimensionless time width of an injection pulse
$T_{d,0}$	Dimensionless hold-up time
u	Linear velocity of a mobile phase
V_i	Elution volume at an elution point i
z	Actual longitudinal distance
Z_d	Dimensionless longitudinal distance
β	Ratio of q_0 to C_0
ϵ	Total porosity of a column

Acknowledgements

This work was supported in part by Grant CHE-97-01680 of the National Science Foundation and by the cooperative agreement between the University of Tennessee and the Oak Ridge National Laboratory. The authors are grateful to Chiral Technologies (Exton, PA, USA) for the generous gift of Chiracel OB stationary phase.

References

[1] G. Guiochon, S. Golshan-Shirazi, A.M. Katti, Fundamentals of Preparative and Nonlinear Chromatography, Academic Press, Boston, MA, 1994.
[2] A.M. Katti, G. Guiochon, Adv. Chromatogr. 31 (1991) 1.
[3] J. Conder, J. Young, in: Physicochemical Measurement by Gas Chromatography, Wiley, New York, 1979, p. 353.
[4] T. Kawai, Kagaku Kogaku Ronbunshu 10 (1984) 513.
[5] S. Golshan-Shirazi, G. Guiochon, Anal. Chem. 61 (1989) 462.
[6] K. Miyabe, G. Guiochon, J. Chromatogr. A 830 (1999) 263.
[7] K. Miyabe, G. Guiochon, J. Chromatogr. A 830 (1999) 29.
[8] K. Miyabe, G. Guiochon, J. Chromatogr. A 857 (1999) 69.

[9] J. Jacobson, J. Frenz, C. Horváth, J. Chromatogr. 316 (1984) 53.
[10] H. Guan, B.J. Stanley, G. Guiochon, J. Chromatogr. A 659 (1994) 27.
[11] S. Khattabi, D.E. Cherrak, J. Fischer, G. Guiochon, J. Chromatogr. A, submitted for publication.
[12] D.E. Cherrak, S. Khattabi, G. Guiochon, J. Chromatogr. A, submitted for publication.